The mechanical and physical ageing of semicrystalline polymers: 1.

L. C. E. Struik
Plastics and Rubber Research Institute TNO, PO Box 71, 2600 AB Delft, The Netherlands
(Received 11 June 1986; accepted 7 April 1987)

A number of commercial semicrystalline polymers have been investigated for ageing effects occurring after quenching from a high temperature T_0 to various temperatures between -170°C and T_0; generally T_0 was kept above 100°C. Before testing the samples were annealed overnight at a temperature T_a higher than T_0 in order to stabilize the crystallinity. After quenching the mechanical creep properties (torsion) as well as the volume relaxation were measured as functions of the time t_e elapsed after quenching. The semicrystalline polymers showed strong ageing effects at temperatures below as well as above the conventional glass transition temperature T_g of the material. These effects could be described in detail using the model of an extended glass transition, introduced several years ago[1]. It is assumed that the crystalline phase reduces the segmental mobility in the amorphous phase, the more so the closer to the crystal surface. Therefore, the amorphous phase no longer has a single T_g but a T_g-distribution. The experiments suggest that the upper T_g, T_g^U, may be much higher (>100°C) than the lowest, T_g^L. Furthermore, the temperature range should be divided in four characteristic regions: Region 1 ($T < T_g^L$), Region 2 ($T \sim T_g^L$), Region 3 ($T_g^L < T < T_g^U$) and Region 4 ($T \geqslant T_g^U$). In these four regions, the ageing and mechanical behaviour is typically different.

(Keywords: semicrystalline polymers; filled rubbers; extended glass transition; physical ageing; creep properties; time–temperature superposition; T_g distribution)

Some years ago[1], a new model for semicrystalline polymers was presented (see *Figure 1*). The main feature of this model is that the crystals disturb the amorphous phase and reduce the segmental mobility. This reduction will be at its maximum in the immediate vicinity of the crystals, and only at large distances from the crystals will the properties of the amorphous phase become equal to those of the bulk amorphous material. This picture was derived from a similar and well-known model for filled rubbers[2–4], in which the carbon black particles restrict the mobility of parts of the rubbery phase.

The main consequence of this immobilization is that the glass transition will be extended towards the high-temperature side. Above the T_g of the bulk amorphous material, some parts of the amorphous phase are rubber, others are glassy, and still other parts will just be passing their glass transition. Consequently, the loss peak (tan δ) at T_g will be extended towards the high-temperature side (*Figure 1*). Concerning physical ageing[1], the model predicts the following: below T_g, the amorphous phase will be completely glassy and suffer from the same ageing effects as a purely amorphous polymer. Above T_g, part of the amorphous phase of the semicrystalline polymer is still glassy. So, for such materials, ageing will persist at temperatures above T_g, a behaviour not exhibited by purely amorphous polymers. This ageing below as well as above T_g has been previously decribed briefly[1]. In a more recent paper[5], it has been shown that the model could be used successfully to analyse the important problem of the ageing of polypropylene[6–11] during long-term storage at room temperature in an inert atmosphere in the dark.

The results of a comprehensive study on 14 different materials, including filled rubbers (c.f. *Figure 1*) will be described in a sequence of papers of which this is the first. It describes the experimental techniques, the materials and the results obtained with respect to the effect of physical ageing on creep properties. It will be shown that the predictions of the model agree with experiment to a detailed degree. Some complementary results are given in the accompanying paper and these refer to dynamic mechanical properties and to the ageing of filled rubber systems. The third paper in the series will deal with the prediction of the long-term creep of semicrystalline polymers and the fourth will deal with the effect of processing (injection moulding vs. compression moulding) on the ageing and creep properties of polypropylene, PP, and HDPE. A general discussion of all of the results will be postponed to the fourth paper in the series.

EXPERIMENTAL

A survey of the materials investigated is given in *Table 1*. Before testing, the sheets and later also the specimens machined from the sheets, were annealed so as to reduce the frozen-in stresses and to achieve a stable state of

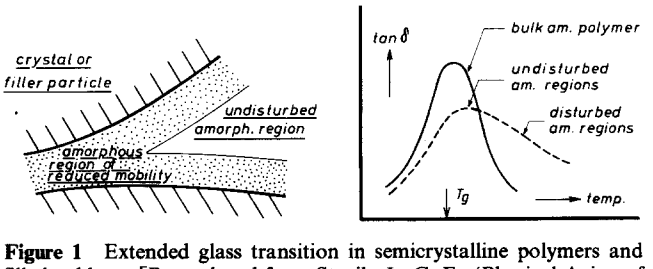

Figure 1 Extended glass transition in semicrystalline polymers and filled rubbers. [Reproduced from Struik, L. C. E., 'Physical Aging of Amorphous Polymers and Other Materials', Elsevier, Amsterdam, 1978, by permission of Elsevier Science Publishers©]

0032-3861/87/091521-13$03.00

Table 1 Summary of materials investigated[a]

Material	TNO code no.	Supplier	Trade name	Density[b] at 23°C (g cm^{-3})	Crystallinity[c] (%)	Annealing temperature, T_a (°C)
LDPE	41	Shell	–	0.9211	45	90
HDPE	40	DSM	Stamylan 9400	0.9655	76	110
POM	42	Philips	Delrin 500	1.427	–	90
PP	43	ANIC	Kastilene M260	0.9118	72	135
PP	61	Rhône-	Napryl 62600	0.9108	71	130
High mol wt PP	62	Progil	Napryl 6204 I	0.9095	69	130
PET	37	Akzo	Arnite A-200	1.3805	38	165
Nucleated nylon-6	59	Montedison	Renyl MV/A	1.1396	30	165
Unnucleated nylon-6	60	Montedison	Renyl MV/E	1.1317	24	165
Nylon-12[d]	38	Hüls	Vestamid L1901	1.0210	~40	160
SBR–HAF	49	TNO	–	–	–	50
Unfilled SBR	55	TNO	–	–	–	70
SBR–HAF	56	TNO	–	–	–	70
SBR–$BaSO_4$	58	TNO	–	–	–	70

[a] The materials, except for the rubbers (49), (55), (56) and (58), were received as sheets compression moulded by the supplier
[b] Measured by hydrostatic weighing in distilled water; accuracy ± 0.0002 g cm^{-3}
[c] Estimated from density, according to the methods described in ref. 12
[d] Also reported are tests on a sample annealed at 90°C; density 1.010 g cm^{-3}, crystallinity ~30%

crystallinity. The annealing was performed in a vacuum oven during one night at the temperatures, T_a, given in *Table 1*. After annealing the materials, still in the vacuum oven, were cooled to room temperature in about 5 h. The nylon samples were carefully dried, and kept dry during the measurements.

Materials

Polypropylene, PP (61)* has a molecular weight comparable with that of PP (43); whilst that of PP (62) is much higher. For PPs (43), (61) and (62), the flow rates according to ASTM specification 1238 are, respectively, 4.8, 6 and 0.4 g/10 min.

The three SBR rubbers (55), (56) and (58) have the same rubbery matrix (100 phr Cariflex S 1500, 5 phr ZnO, 2 phr stearic acid, 1.5 phr Flectol H, 1.75 phr sulphur and 1.25 phr Santocure). Rubber (55) is unfilled, rubber (56) contains 82.6 phr (i.e. 30 vol%) HAF black, rubber (58) is filled with 200 phr (i.e. 30 vol%) $BaSO_4$. Rubber (49) has the composition: 100 phr Cariflex S 1500, 50 phr HAF, 3 phr ZnO, 1 phr stearic acid, 5 phr Dutrex 55, 1.25 phr CBS and 2 phr sulphur.

PREDICTIONS OF THE MODEL WITH RESPECT TO AGEING AND CREEP

Before discussing the experimental results obtained on the materials in *Table 1*. we will first analyse what the model shown in *Figure 1* actually predicts with respect to ageing, creep, dynamic mechanical properties and volume relaxation. The comparison of predictions with experiment is given in the following section† ('Comparison of predictions with experiment').

The role of the crystalline phase

To elaborate the model, we must know whether the viscoelasticity of the semicrystalline material is entirely due to contributions from the amorphous phase, or whether there are also contributions from the crystalline phase. Since there is no *a priori* answer to this question, we begin by assuming that the crystalline phase does not contribute to the viscoelasticity, that it behaves elastically, and that the degree of crystallinity remains constant. In other words, we assume that the crystalline phase acts as an 'inert' filler, and we investigate to what extent these assumptions can explain the behaviour of the material. Thus the approach is: start with the most simple assumption and see how it works.

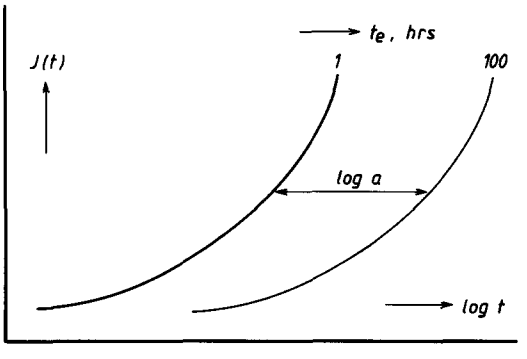

Figure 2 Effect of physical ageing on the small-strain creep of an amorphous polymer quenched from a temperature $T_0 > T_g$ to $T < T_g$. t_e is the time elapsed at T after the quench; $J(t)$ is the creep compliance in shear. The prime effect of ageing is a shift of the creep curves (horizontally) along the log (creep) time scale. The shift, relative to the creep curve at some reference value of t_e, is denoted by $\log a$, the shift rate by $\mu = \mathrm{d} \log a / \mathrm{d} \log t_e$. Schematic from ref. 1

Summary of the behaviour of amorphous polymers (ref. 1)

The model in *Figure 1* and the 'inert filler' assumption discussed above imply that the viscoelastic and ageing behaviour of semicrystalline polymers is due entirely to the amorphous phase. We therefore start by summarizing the behaviour of purely amorphous polymers. An outline of the effects of temperature and ageing on creep (viscoelasticity) is given in *Figures 2* and *3*.

Below T_g, amorphous glassy polymers show the so-called ageing range. The upper temperature limit is T_g, the lower limit is T_β of the highest secondary transition. In

* Numbers in brackets are TNO code numbers, these differ from those in Appendix B of ref. 1.
† As usual the 'predictions' were made after having obtained the experimental results. The reason for giving the theory first is the complexity of the empirical findings; it is useful to have some framework by which the empirical findings can be rationalized.

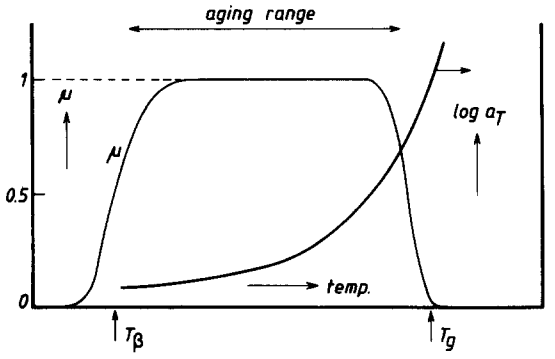

Figure 3 Effect of temperature T on ageing and creep of an amorphous polymer quenched from $T_0 > T_g$ to $T < T_g$. Shift rate μ is defined in the legend to *Figure 2*. Log a_T is the (thermal) shift between creep curves measured at different temperatures but at a constant value of ageing time t_e. T_β is the temperature of the (highest) secondary transition (lower limit of the ageing range)

this range, the material shows the following behaviour characteristics:

(a) The creep curves* have a high positive curvature approximately obeying the equation:

$$J(t) = J_0 \exp[(t/t_0)^\gamma] \quad (1)$$

where J_0 and t_0 are constants dependent on temperature and ageing time, while γ is about 1/3.

(b) The creep curves measured at different temperatures can be superimposed by horizontal and vertical shifts in a double-logarithmic diagram (this is implied in equation (1); the horizontal shifts are due to the changes in $\log t_0$, the vertical shifts to those in $\log J_0$).

(c) Ageing affects the creep curves by shifts that are almost horizontal. The double-logarithmic shift rate μ is about unity, and it decreases to zero at T_g and at the low-temperature end of the ageing range (roughly at the first secondary transition T_β, see *Figure 3*).

(d) At temperatures sufficiently below T_g, the effect of temperature on creep is small. The 'retardation time' t_0 in equation (1) increases nearly proportionally to $T_g - T$, and so the log a_T vs. T curve shown in *Figure 3* flattens at low temperatures. The origin of this non-Arrhenius behaviour has already been discussed previously[1].

When the temperature approaches T_g, the behaviour of the material changes. The thermal shifts, log a_T, begin to increase rapidly, and the ageing rate μ decreases to zero (see *Figure 3*). Moreover, the shape of the creep curves begins to change, and this is illustrated in *Figure 4*.

For short times or temperatures at the lower side of the glass–rubber transition (i.e. as long as $J < 10^{-8}$ m^2/N), the creep curve still obeys equation (1), and the double-logarithmic creep rate $m = \mathrm{d} \ln J(t)/\mathrm{d} \ln t$ increases according to†:

$$\frac{\mathrm{d} \ln m}{\mathrm{d} \ln t} = \gamma \sim 1/3 \quad (2)$$

which follows from equation (1) by differentiation with respect to t.

* The entire paper deals with short-time momentary compliances[1], i.e. the creep time remains much shorter than the elapsed ageing time t_e; therefore, the creep is not affected by simultaneous ageing.

† $\ln x = {}^e\log x$; $\log x = {}^{10}\log x$.

For longer times, the material enters the central part of the glass transition; equation (1) is no longer obeyed and m remains almost constant for 2–3 decades. The maximum slope m_1 depends on the structure of the polymer and generally ranges from 0.50–0.75, its theoretical limit being unity[13]. For still longer times, the glass–rubber transition is completed, and the material reaches the pseudo-equilibrium rubbery plateau region. Slope m decreases to a value of the order of 0.05–0.10 (see *Figure 4*), and when plotted in a double-logarithmic diagram $J(t)$ will follow a more or less straight line. Naturally, this only holds when there are sufficient physical or chemical crosslinks to prevent viscous flow, a condition that for semicrystalline polymers is fulfilled since the crystallites act as crosslinks.

Semicrystalline materials; the four characteristic temperature regions

We will now derive the creep and ageing behaviour of semicrystalline polymers from the behaviour of amorphous polymers (as summarized in the above section) combined with the concept of a distribution of T_g's. For simplicity, we model the distribution of T_g's by assuming that there are only two clearly distinct T_g's (compare *Figure 5*). The most mobile regions have the lowest T_g, viz. T_g^L, the less mobile regions have a T_g equal to $T_g^U > T_g^L$. We further assume that the creep compliance $J(t)$ is simply the sum of a contribution $J_1(t)$ of the most mobile regions and a contribution $J_2(t)$ of the less mobile regions (this is of course an approximation, made for simplicity):

$$J(t) = J_1(t) + J_2(t) \quad (3)$$

To establish the properties of the semicrystalline polymer, we apply what was discussed in the previous section by merely 'adding' the behaviour of two amorphous

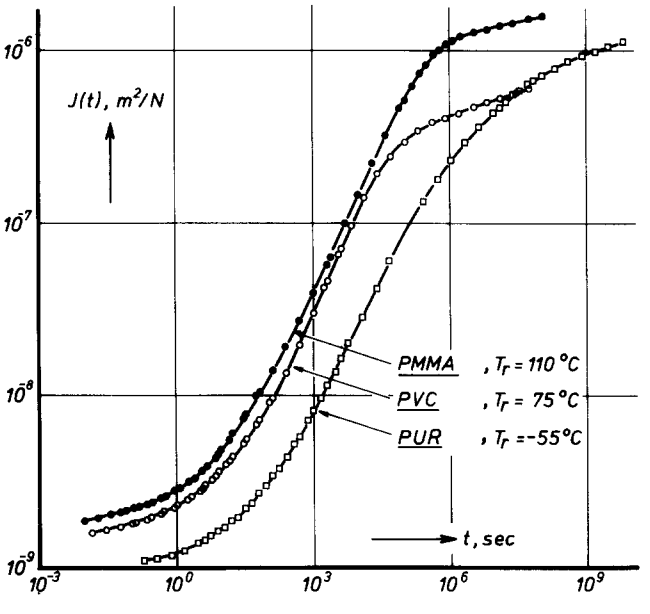

Figure 4 Behaviour in the glass–rubber transition range. Master creep curves obtained by time–temperature superposition. The original curves were measured 3 h after quenches from 160°C (PMMA), 150°C (PVC) and 60°C (PUR) to various temperatures T; T_r is the reference temperature. PMMA and PVC were the materials 24 and 3 of Appendix B of ref. 1; the unfilled polyurethane rubber is the same material as used in ref. 3

polymers with different T_g's (T_g^L and T_g^U). As indicated in *Figure 5* this leads to a division of the temperature scale in four characteristic regions of behaviour: Region 1 ($T < T_g^L$), Region 2 ($T \sim T_g^L$), Region 3 ($T_g^L < T < T_g^U$) and Region 4 ($T \geqslant T_g^U$) and these regions will now be discussed singly. A summary of the results is given in *Figure 8*.

Region 1 ($T < T_g^L$). In this temperature range, both amorphous regions are below their respective T_gs. As the upper limit of Region 1 we take the temperature (close to T_g^L) at which the contribution $J_1(t)$ begins to deviate from equation (1). At this temperature the creep of the more mobile regions enters the central part of the glass transition (compare with *Figure 4*).

At temperatures well below T_g^L, both amorphous regions have a modulus comparable with the glassy modulus of amorphous polymers. This means that the semicrystalline polymer has a shear modulus of at least 10^9 N/m^2. Furthermore the compliances in both amorphous regions obey equation (1), the mechanical retardation times being about equal (see log a_T curves in *Figure 5*), and also the shift rate μ will be the same (i.e. equal to unity, see *Figure 5*). Consequently, *at temperatures well below T_g^L, the creep and ageing behaviour of the semicrystalline polymer will be similar to that of amorphous polymers* (see aspects (a)–(d) in the previous section.

In the upper part of Region 1 (i.e. near T_g^L), the behaviour is different. The contribution $J_1(t)$ of the more mobile regions begins to shift more rapidly with temperature than $J_2(t)$ (see *Figure 5*). Consequently, the contributions $J_1(t)$ and $J_2(t)$ are pulled apart on the time scale. This implies that, since the creep rate strongly increases with time (see equations (1) and (2)), the curvature (i.e. the shape) of the total creep curve becomes dominated by the contribution $J_1(t)$. However, by definition (see above), $J_1(t)$ obeys equation (1) up to the upper limit of Region 1. Therefore, the same will hold, approximately, for the total compliance $J(t)$ (the shape of $J(t)$ is dominated by that of $J_1(t)$, see above). Consequently, time–temperature superposition is applicable over the entire Region 1; the thermal shifts log a_T will be small at low temperatures and begin to accelerate when T_g^L is approached (see *Figure 8*).

Let us now consider the ageing effects near T_g^L (see *Figure 6a*). In the vicinity of T_g^L, the shift rate μ of $J_1(t)$ decreases with increasing temperature whereas that of $J_2(t)$ remains at unity (*Figures 5* and *6a*). At the same time, the shape of $J(t)$ becomes dominated by that of $J_1(t)$ (see *Figure 6*) which means that the curvature $d^2J_2/d\ln t^2$ is much less than $d^2J_1/d\ln t^2$. Suppose, for simplicity, that we can neglect the curvature of $J_2(t)$, i.e. that we can approximate $J_2(t)$ by a straight line on log time scale (*Figure 6b*). This straight line shifts to the right by ageing (shift *b* in *Figure 6b*), but for straight lines, horizontal shifts are indistinguishable from vertical shifts (shift *c* in *Figure 6b*). Consequently, the effect of ageing on the total compliance $J(t)$ can be conceived of as a horizontal shift due to the effect on $J_1(t)$ (shift *a* in *Figure 6b*), combined with a (downward) vertical shift due to the effect on $J_2(t)$ (shift *c* in *Figure 6b*). Therefore, the creep curves measured

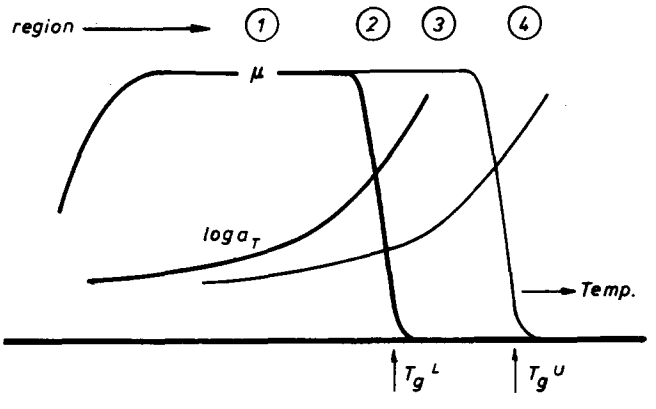

Figure 5 Effect of ageing and temperature on the creep in two amorphous regions with T_gs equal to T_g^L (——) and T_g^U (– – –). μ is the shift rate d log a/d log t_e, characterizing the isothermal ageing; log a_T denotes the thermal shifts at a constant value of t_e. Because of the different T_gs, the μ- and log a_T plots of the two regions are different (—— and – – –). Note that the word 'region' is used in two ways: an amorphous region is a part of the material; the Regions 1–4, indicated in the top of the diagram are regions on the temperature scale

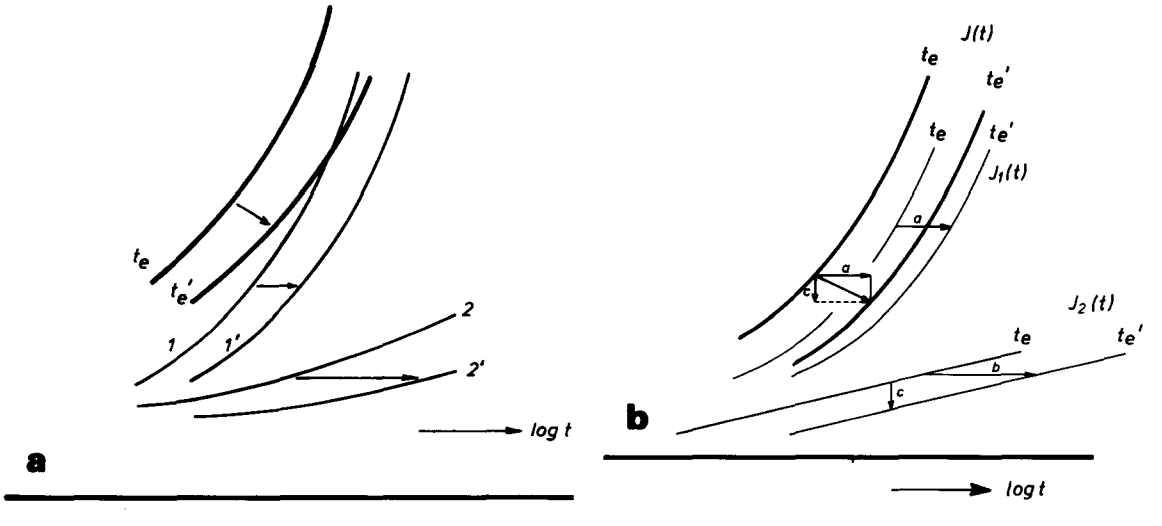

Figure 6 (a) Effect of ageing on the creep in the high temperature part of Region 1, and on that in Region 2. Curves 1 and 1' refer to the more mobile, curves 2 and 2' to the less mobile amorphous regions. Curves 1 and 2 refer to an ageing time t_e, curves 1' and 2' to a time $t_e' > t_e$. The heavy curves are the total compliances $J(t) = J_1(t) + J_2(t)$ for the ageing times t_e and t_e'; the shifts produced by ageing are indicated by arrows. (b) The limiting case in which the curvature of $J_2(t)$ can be neglected with respect to that of $J_1(t)$; for details see text

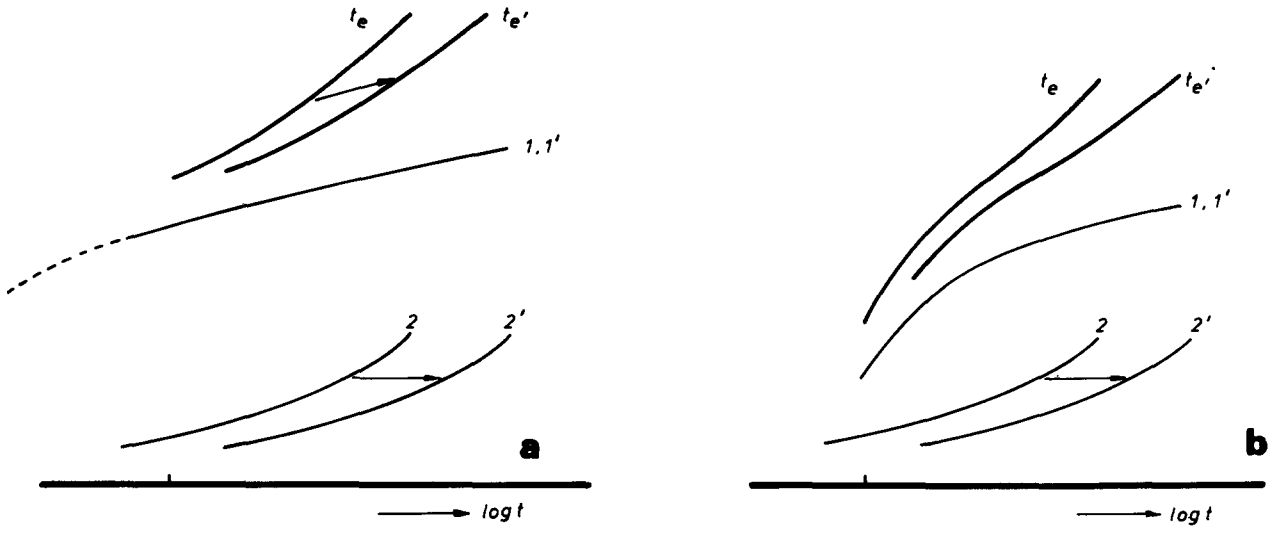

Figure 7 As for *Figure 6*, but now for Region 3. For explanaton and for the difference between (a) and (b) see text

at different values of t_e can be superimposed by horizontal and downward vertical shifts in a semi-logarithmic diagram. The horizontal shift rate μ is determined by the shifting of $J_1(t)$; which will be smaller than unity and will decrease with increasing temperature (compare with *Figure 8*). The downward shifts will be small or zero at $T \ll T_g^L$, but will increase in importance when T_g^L is approached (*Figure 8*).

Region 2 ($T \sim T_g^L$). Around T_g^L, there is a narrow temperature range in which (i) the shape of $J(t)$ is still largely determined by that of $J_1(t)$, (ii) $J_1(t)$ no longer obeys equation (1), (iii) $J_1(t)$ is still affected by ageing. These conditions will be fulfilled at those temperatures at which $J_1(t)$ enters the central part of the glass transition. As shown in *Figure 8* and explained in *Figure 6*, the behaviour in Region 2 is very similar to that in the high-temperature part of Region 1. Ageing produces horizontal plus downward vertical shifts and the shift rate μ continues to decrease with temperature. The thermal shifts $\log a_T$ are large, and in fact, the only difference from Region 1 is that the creep curve no longer obeys equation (1) and its long-time end will be flattened (see *Figure 8*).

Region 3 ($T_g^L < T_g < T_g^U$). In this temperature range $J_1(t)$ has reached the end of the glass–rubber transition or the pseudo-equilibrium plateau region (*Figure 4*) and it is no longer sensitive to ageing; all ageing effects therefore arise from those in $J_2(t)$.

The ageing behaviour will be simplest at temperatures well above T_g^L, i.e. at temperatures at which $J_1(t)$ has reached the pseudo-plateau region and only varies slowly with time. Ageing produces horizontal shifts of $J_2(t)$, but as shown in *Figure 7a*, the total compliance $J(t) = J_1(t) + J_2(t)$ will shift upward to the right, at least in a semi-logarithmic diagram and when $J_1(t)$ follows a straight line on the log t scale. The horizontal component μ of the shift rate of $J(t)$ is determined by the shifting of $J_2(t)$; at temperatures sufficiently below T_g^U it will be about unity. The vertical shift rate is determined by the slope of $J_1(t)$.

Complications arise in the low temperature side of Region 3, i.e. at temperatures in the vicinity of T_g^L. First of all there will be a narrow temperature range in which $J_1(t)$

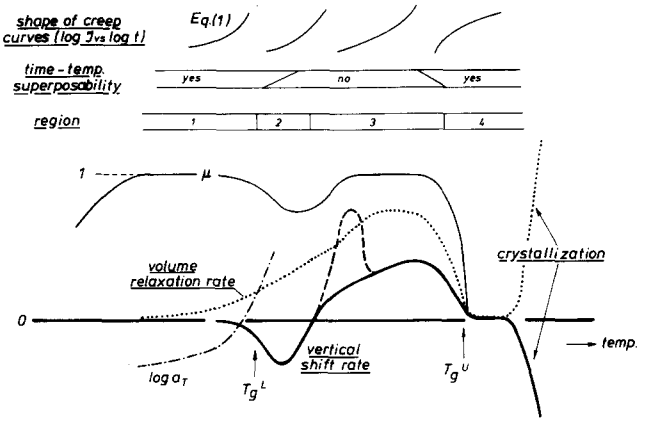

Figure 8 Creep, ageing and volume relaxation behaviour of semicrystalline polymers as predicted by the model

has not yet reached the pseudo-plateau region although it is already insensitive to ageing. In a semi-logarithmic diagram, $J_1(t)$ again follows a straight line (at least approximately), the slope of which, however, is much greater than in the pseudo-plateau region. As before, ageing produces horizontal and upward vertical shifts, the vertical shift rate, however, being very large (see the broken line in *Figure 8*; this case is not shown in *Figure 7*).

Slightly above the temperature range mentioned above, $J_1(t)$ will just be leaving the glass transition. The $J_1(t)$ vs. log t curve has a bend at which its slope decreases (see *Figure 7b*). The result is that the effects of ageing on the total compliance become very complicated, and can no longer be deconvoluted into horizontal and vertical shifts.

The shapes of the creep curves in the upper part of Region 3 is indicated in *Figure 8*. An upswing, that is due to the creep of the less mobile regions, is superimposed on the 'pseudo-equilibrium' creep of the more mobile regions (see *Figure 7a*). The creep curve is rather flat at short times, and a region of positive curvature is found on the long-time side (exactly the reverse of the behaviour in Region 2). The effect of temperature on the creep in Region 3 will be discussed in the next section.

Region 4 ($T \geqslant T_g^U$). In this region, the entire amorphous phase becomes rubbery. The ageing effects disappear, the

horizontal and vertical shift rates tend to zero, and the material shows the normal behaviour of a polymer above its T_g. The shape of the creep curve is shown in *Figure 8*; the slope of $J(t)$ decreases with time and at longer times $J(t)$ enters the pseudo-equilibrium range.

However, for this simple model with only two T_g's, the actual situation is somewhat more complex in at least two respects:

(*a*) *A distribution of T_g's.* The T_g's of the different amorphous regions are distributed over the entire interval between T_g^L and T_g^U. However, as we will see in the following, this does not basically change the behaviour. In Region 1, all amorphous regions will be glassy. At higher temperatures, we will first have a range in which the shape of the creep curve is determined by the contributions of the more mobile regions. As was discussed previously, ageing produces horizontal and downward vertical shifts, and the horizontal shift rate μ decreases with increasing temperature. At still higher temperatures, the more mobile regions become rubbery, the shape of the creep curve being determined by the less mobile regions, and consequently a type 3 behaviour must be expected. Finally, when the temperature is increased still further, all amorphous regions become rubbery, and the ageing effects disappear (Region 4). We thus conclude that the distribution in T_g's does not alter the qualitative distinction between the four different regions of behaviour; the only change may be that the transition from one region to another becomes more gradual.

(*b*) *Crystallization.* In Region 4, the most immobilized amorphous regions, i.e. those in the immediate vicinity of the crystals, will become rubbery. This implies that crystallization processes, which were hardly possible in Regions 1–3, now become possible, and may give rise to additional ageing effects. These will differ in nature from those discussed so far, in that, to a first approximation, the creep curve will not change its position on the time scale ($\mu=0$). When $J(t)$ is plotted in a double-logarithmic diagram, the changes in crystallinity are revealed as downward vertical shifts (stiffening by an increase in the degree of crystallinity).

A recapitulation of the results obtained so far is given in *Figure 8*. We have found that there are four characteristic temperature regions. In Region 1 the behaviour equals that of an amorphous polymer. The creep curve obeys equation (1), and at low temperatures ageing produces almost horizontal shifts with the shift rate μ being about unity. At higher temperatures, the shifts are increasingly accompanied by downward vertical shifts and μ begins to decrease. This behaviour continues in Region 2, and the only difference between Regions 2 and 1 is that in the former the creep curve no longer obeys equation (1). At higher temperatures, we have Region 3, characterized by the fact that the horizontal shifts are accompanied by upward vertical shifts. At still higher temperatures (Region 4), the ageing effects disappear or change in nature (crystallization).

Effect of temperature on creep

The effect of temperature on creep will vary strongly between the different temperature regions. As discussed before, we expect time–temperature superposability in Regions 1, 2 and 4, but in Region 3, the behaviour will be more complicated (see *Figure 9*). With increasing temperature, more and more amorphous material becomes rubbery. The polymer becomes softer, and the upswing in the creep curve at long times, that is due to the still glassy amorphous regions, becomes less pronounced. *This flattening of the creep curves implies that time–temperature superposition is no longer possible.*

A typical feature of Region 3 is that, with increasing temperature, the upswing in the creep curve hardly changes its position on the time scale (*Figure 9*). A tentative explanation may be that the upswing is due to the creep of the less mobile layers. However, since the polymer is much softer than in Region 1, these layers will only contribute significantly to the total creep compliance when their creep is very pronounced, i.e. when they are at the beginning or just passing their glass transition. This means that, at all temperatures in Region 3, the upswing is due to layers just arriving at their T_g. By definition, relaxation times are always the same at T_g, i.e. equal to the experimental time scale. Consequently, the position of the upswing (*Figure 9*) on the time scale will hardly change with temperature. If time–temperature superposition were possible, the main effect of temperature would be a vertical instead of a horizontal shifting.

Modulus and damping

According to linear viscoelastic theory[13], the dynamic modulus $G'(\omega)$ and damping $\tan\delta(\omega)$, both at an angular frequency ω, can be calculated to a good approximation from creep compliance $J(t)$ by:

$$G'(\omega)\simeq 1/J(t) \quad ; \quad t=1/\omega \tag{4}$$

$$\tan\delta(\omega)\simeq\frac{\pi}{2}\frac{\mathrm{d}\ln J(t)}{\mathrm{d}\ln t}=\frac{\pi}{2}m \quad ; \quad t=1/\omega \tag{5}$$

Consequently, the dynamic behaviour can be derived from the creep properties.

At the end of Region 1, m and $\tan\delta$ are increasing with temperature whilst in Region 4, they will be decreasing. Therefore, one or more maxima in $\tan\delta$ must be found between T_g^L and T_g^U. If there are two well distinguished glass transitions (see *Figure 5*), $\tan\delta$ will pass through two peaks, one located around T_g^L, and the other around T_g^U. If there is a distribution of T_g's, all possibilities, varying from a single peak, or a peak with a shoulder, to two peaks may be realized. The relative intensities of the low and high temperature peaks will depend on the degree of immobilization of the amorphous phase. An increase in immobilization, e.g. by an increase in the

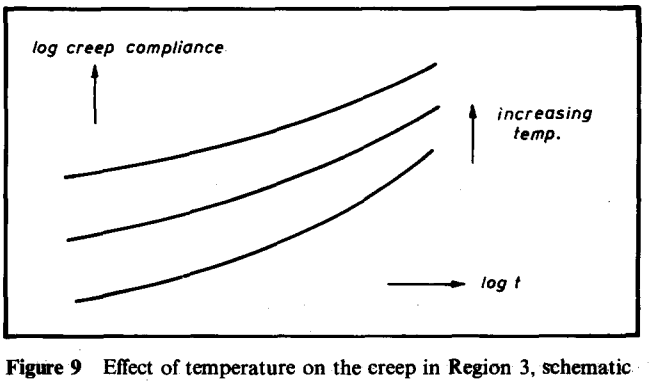

Figure 9 Effect of temperature on the creep in Region 3, schematic

degree of crystallinity, will reduce the low temperature peak and raise the high-temperature peak.

Volume relaxation

In amorphous polymers, the volume relaxation rate $\beta = (-1/v)\mathrm{d}v/\mathrm{d}\log t_e$ passes through a maximum just below T_g (see e.g. Appendix A.2 of ref. 1). Therefore it should be expected that, in semicrystalline materials, β will also show a maximum. This maximum will be found at that temperature, in either Region 2 or 3, where most of the amorphous phase is passing through its T_g (compare with *Figure 8*). At lower temperatures, i.e. in Region 1, the material behaves as an amorphous polymer. In the ageing range, the volume relaxation rate β monotonically increases with temperature, and the value of β can be estimated from the behaviour of amorphous polymers. Below their T_gs, these materials show β's of at most 8×10^{-4}/decade. In crystalline polymers, the crystalline phase is supposed not to contribute to β. Since the degree of crystallinity generally ranges from 30–80%, we therefore expect a β of at most $2\text{–}6 \times 10^{-4}$/decade.

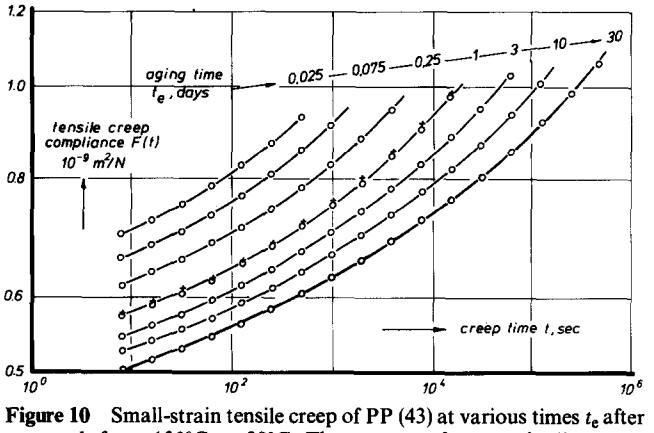

Figure 10 Small-strain tensile creep of PP (43) at various times t_e after a quench from 120°C to 20°C. The crosses refer to a duplicate test (requenching) done on the same specimen after completion of the first series of measurements. In this duplicate test, the measurements at t_e's of 0.025, 0.075 and 0.25 days were omitted. [Reproduced from Struik, L. C. E., 'Physical Aging of Amorphous Polymers and Other Materials', Elsevier, Amsterdam, 1978, by permission of Elsevier Science Publishers©]

COMPARISON OF PREDICTIONS WITH EXPERIMENT

The semicrystalline materials in *Table 1* were investigated for creep, ageing and volume relaxation. Each individual test was begun with a 30 min heating period to some initial temperature T_0, located a little below the previous annealing temperature T_a (see *Table 1*). The sample was then quenched to the measuring temperature T and the creep curves at T were measured at elapsed times t_e of 0.35–12 h (in some cases 0.60 to 720 h). The volume relaxation between 30 min and 6 h after quenching was determined in the same way. For details concerning the techniques, refer to ref. 1.

Important ageing effects were found at almost all temperatures and in all of the materials. An example on PP is given in *Figure 10*, which shows that at 20°C the changes in compliance are as large as 40–60%. The Figure also shows that the results of the experiment are reproducible, and are not influenced by the fact that the different curves were determined by sequential testing on a single specimen[14].

The general picture given in the previous section (ageing behaviour different in the four different temperature regions) and its agreement with experiment will now be discussed. Illustrations are given in *Figures 11* and *12*, which show the creep of PP and HDPE at various

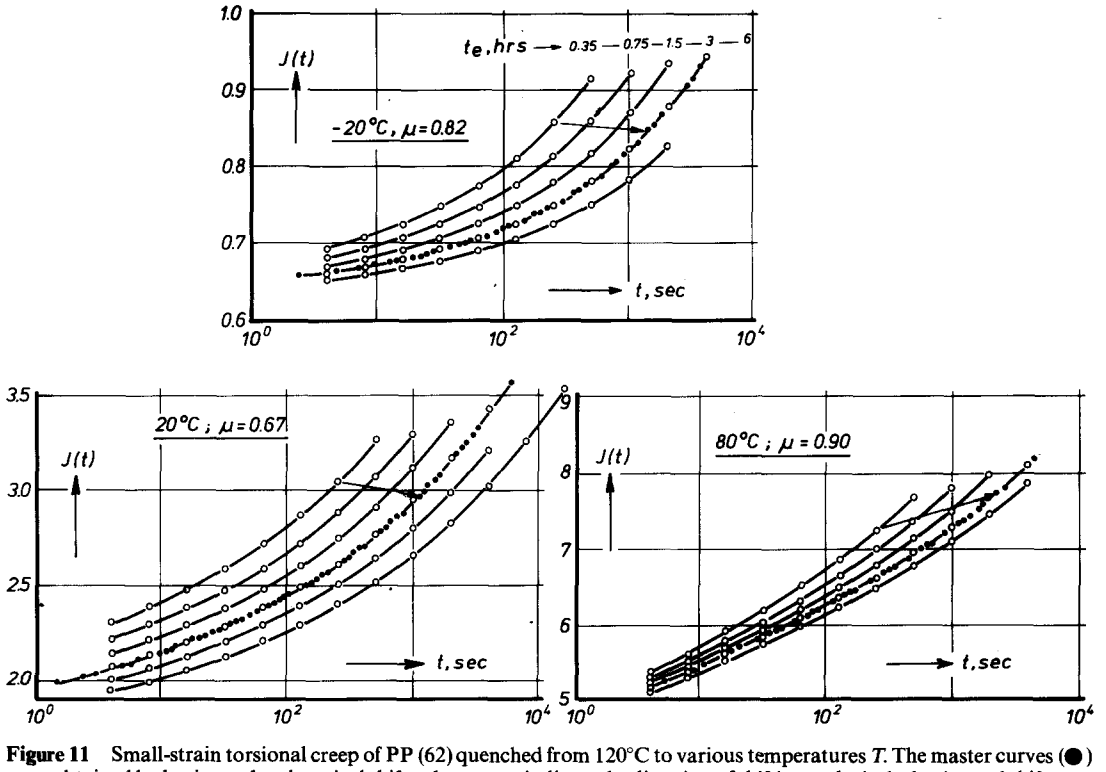

Figure 11 Small-strain torsional creep of PP (62) quenched from 120°C to various temperatures T. The master curves (●) were obtained by horizontal and vertical shifts; the arrows indicate the direction of shifting and μ is the horizontal shift rate. $J(t)$ is expressed in 10^{-9} m²/N. The same sequence of t_e values was used in each test; in some cases the longest t_e-values (6 and 12 h) were omitted. The t_e-values are given in only one of the subfigures

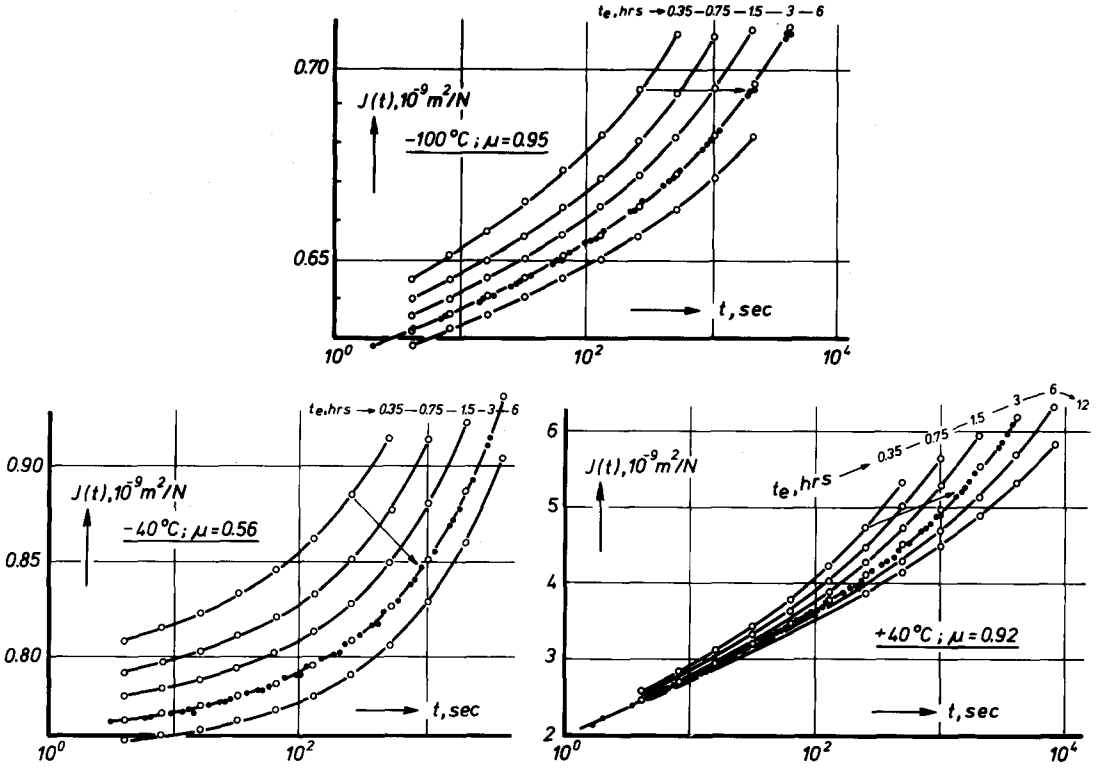

Figure 12 As for *Figure 11*, but now for HDPE (40) quenched from 100°C

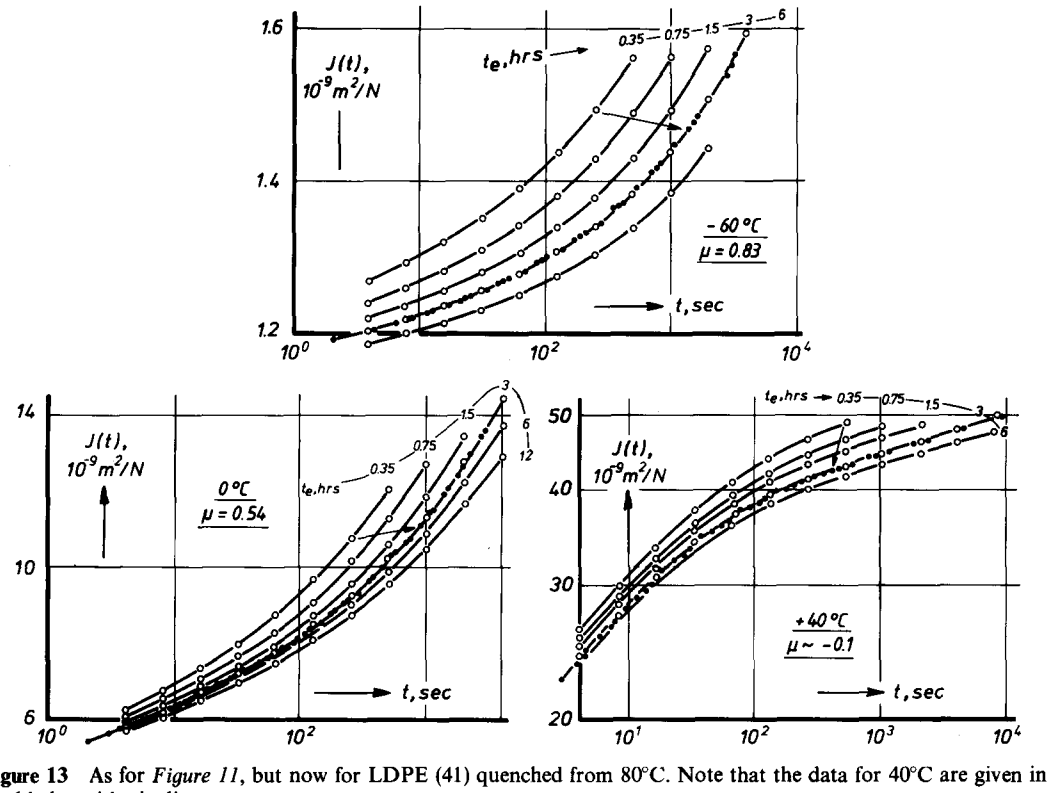

Figure 13 As for *Figure 11*, but now for LDPE (41) quenched from 80°C. Note that the data for 40°C are given in a double-logarithmic diagram

values of temperature and elapsed time. The diagrams are semi-logarithmic and the master curves were obtained by horizontal and vertical shifts. The individual creep curves could always be exactly superimposed.

At low temperatures the shifts are almost horizontal (Region 1 behaviour). At higher temperatures we first have downward vertical shifts (Region 1 or 2 behaviour) and followed by upward and vertical shifts (Region 3 behaviour).

The tests on PP and HDPE were limited to temperatures below 100°C, and Region 4 behaviour could not be observed. However, such behaviour is clearly exhibited by LDPE (see *Figure 13*). For this polymer, the shifts are horizontal at very low temperatures (−100°C, not shown); at −60°C we have downward vertical shifts, and at 0°C the behaviour has changed to type 3. For 40°C and higher temperatures, we have type 4 behaviour and the creep compliance clearly enters the pseudo-plateau

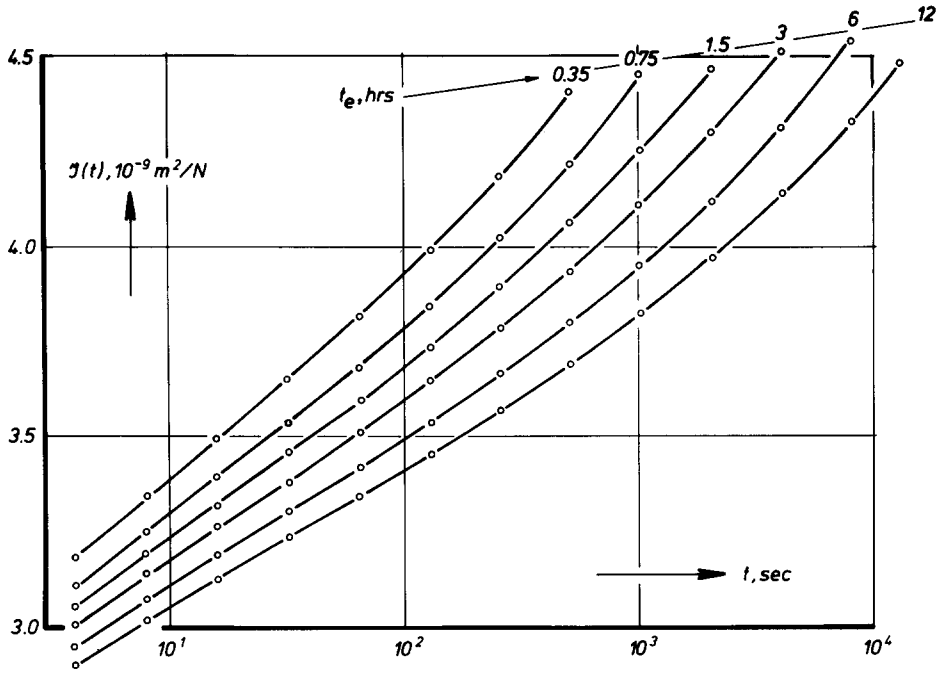

Figure 14 Small-strain torsional creep of nylon-6 (59) at various times t_e, elapsed after a quench from 150°C to 80°C

region. However, in Region 4, the creep is accompanied by marked ageing effects. The creep curves shift almost vertically in a double-logarithmic diagram, and μ is even slightly negative. This ageing is quite probably due to crystallization and arguments for this will be presented later.

In summary, we have indeed found 4 characteristic types of behaviour, and with increasing temperature they appear in the expected order. Moreover, with PP, the T_g of which is well known, the different regions are found where they are expected (see *Figure 12*).

To futher test the model we constructed diagrams similar to *Figure 8*, but based on experimental data, for all the semicrystalline polymers investigated. These diagrams are exhibited in *Figures 19–24*, and give the following information:

(1) The ageing rates μ and β were obtained as follows: The creep curves measured at various values of elapsed time were plotted in semi-logarithmic diagrams. They could nearly always be superimposed by horizontal log shifts $\log a$ and vertical shifts b. The rates μ and B were then calculated by:

$$\mu = \frac{\mathrm{d}\log a}{\mathrm{d}\log t_e} \tag{6}$$

$$B = \frac{1}{J(t_e,t)}\frac{\mathrm{d}b}{\mathrm{d}\log t_e} \quad ; \quad t = 1024\,\mathrm{s}; \quad t_e = 3\,\mathrm{h} \tag{7}$$

Accordingly, B is the relative change in the 1024 s compliance per ten-fold increase in the elapsed time; B is taken as positive for upward vertical shifts.

For LDPE, superposition in semi-logarithmic plots was impossible for $T \geqslant 20$°C. However, good master curves could be obtained by using double-logarithmic diagrams (see *Figure 13*), and from the shift data, rates μ and B could be calculated as before.

For some materials a superposition of the individual creep curves was impossible but only in narrow temperature regions (see e.g. *Figure 14*). In such cases, rates μ and B could not be determined, and in *Figures 19–24* this is indicated by the dashing of the μ vs. T and B vs. T curves. As expected, these difficulties are encountered only at the boundary of Regions 2 and 3; moverover, the way in which, at these temperatures, the creep is affected by ageing, agrees with the predictions (compare *Figures 7b* and *14*).

Further items of information given in *Figures 19–24* are:

(2) Plots of shear modulus G' and damping $\tan\delta$ both at a frequency $\nu = \omega/2\pi$ of 1.55×10^{-4} Hz and calculated using equations (4) and (5) from the creep at $t_e = 6$ h and $t = 1024$ s.

(3) The volume relaxation rate $\beta = (-1/v)\,\mathrm{d}v/\mathrm{d}\log t_e$ in which v denotes the specific volume. Assuming isotropy, we calculated β from length–relaxation data such as that shown in *Figure 15*. After a period of initial curvature, the length l vs. $\log t_e$ curves become almost straight, and β was determined from the slope at $t_e = 10^4$ s. In two cases (PP and LDPE at 23°C), the assumption of isotropy was also confirmed by determining β from density measurements.

(4) Concerning the shapes of the creep curves and the possibilities of time–temperature superposition; according to our model, we distinguished between four types of creep curves:

Type 1—The curves have a high positive curvature and approximately obey equation (1). For all polymers a temperature range of such behaviour could be detected, and in this range, time–temperature superposition appeared to be possible (see *Figure 16*).

Type 2—The creep curves no longer obey equation (1); they are flattened on the long-time side and the time–temperature superposition begins to fail (see *Figure 17*).

Type 3—The creep curves behave as illustrated in *Figure 17*. At longer times, the gradual increase in compliance is accompanied by an upswing, that becomes less marked with increasing temperature. Time–temperature superposition is no longer possible (compare with *Figure 9*).

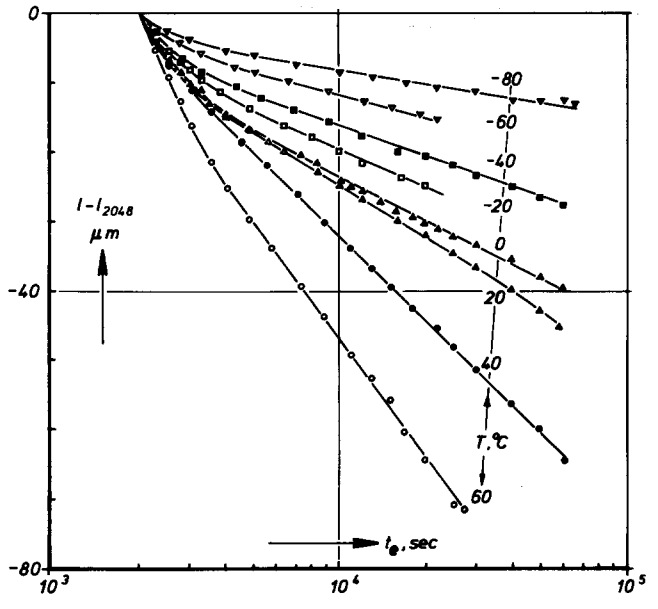

Figure 15 Length relaxation of LDPE (41) quenched from 80°C to various temperatures T. The time elapsed after quenching is denoted by t_e; l is the momentary length of the sample, l_{2048} the length at $t_e = 2048$ s

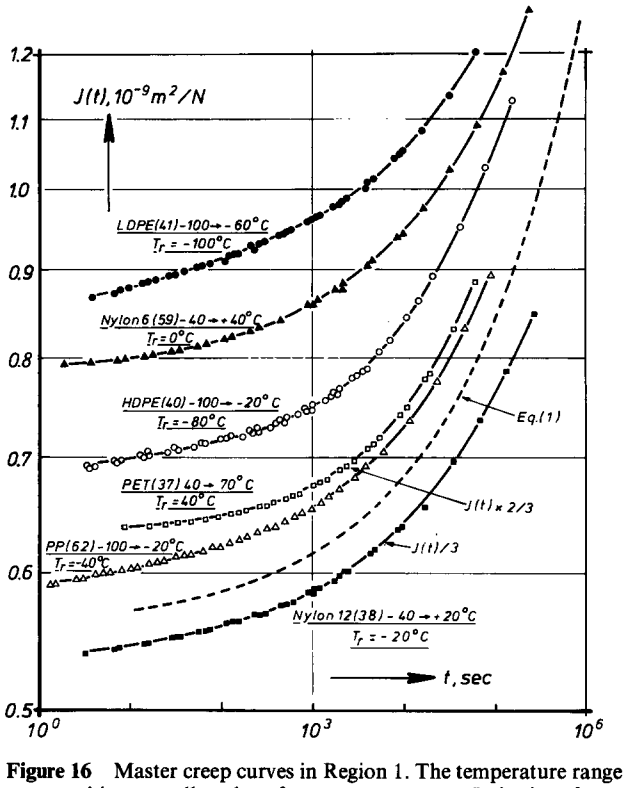

Figure 16 Master creep curves in Region 1. The temperature range of superposition as well as the reference temperature, T_r, is given for each material. The broken curve obeys equation (1); its position has been chosen arbitrarily. The t_e value is 3 h

Type 4—The material behaves as an amorphous polymer at the high-temperature side of its glass transition. At short times the logarithmic creep rate is large, but at longer times the compliance enters the pseudo-plateau region (see *Figure 18*). Time–temperature superposition is again possible.

As regards these shape characteristics, it should be realized that Region 1 or Region 4 behaviour can be recognized unambiguously. The distinction between Regions 2 and 3 is more difficult, and in general the change in behaviour from type 2 to type 3 is gradual (see *Figure 17*).

(5) The thermal acceleration $\log a_T$. The final piece of information given in *Figures 19–24* concerns the thermal acceleration of the creep in those regions (1, 2 and 4) where time–temperature superposition is possible. The horizontal shift factor $\log a_T$ relative to some arbitrary reference temperature T_r is plotted as a function of temperature.

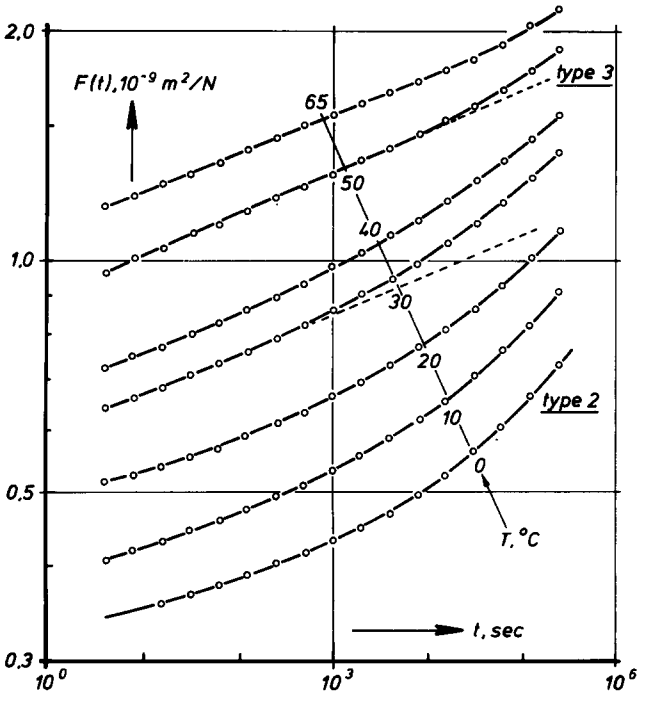

Figure 17 Tensile creep of PP(43) started at a t_e of 10 days after a quench from 120°C to T. At 0°C and 10°C, the curves are of type 2; above 30°C they are of type 3. The broken lines are linear extrapolations

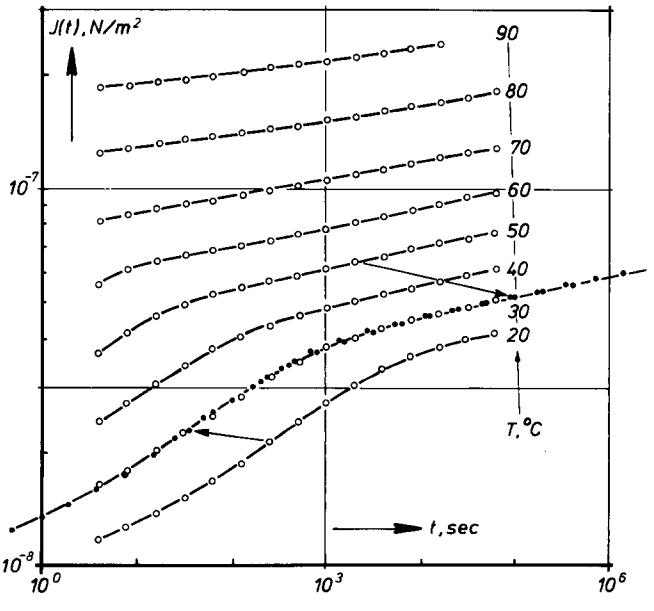

Figure 18 Small-strain torsional creep of LDPE (41). The tests were started 30 min after quenches from 95°C to T. The master curve was obtained by superposing the data at 20°C–50°C

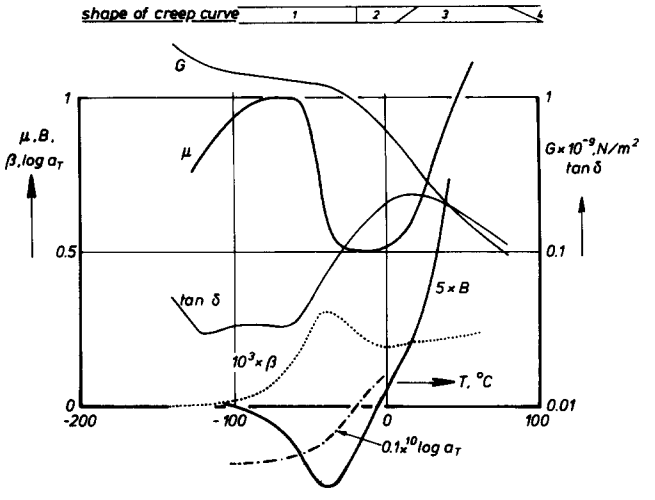

Figure 19 Creep, ageing and volume relaxation behaviour of HDPE (40), quenched from 100°C to various temperatures T. Also given are the dynamic modulus G' and damping $\tan\delta$ at 1.55×10^{-4} Hz as derived from the creep data. For details see text

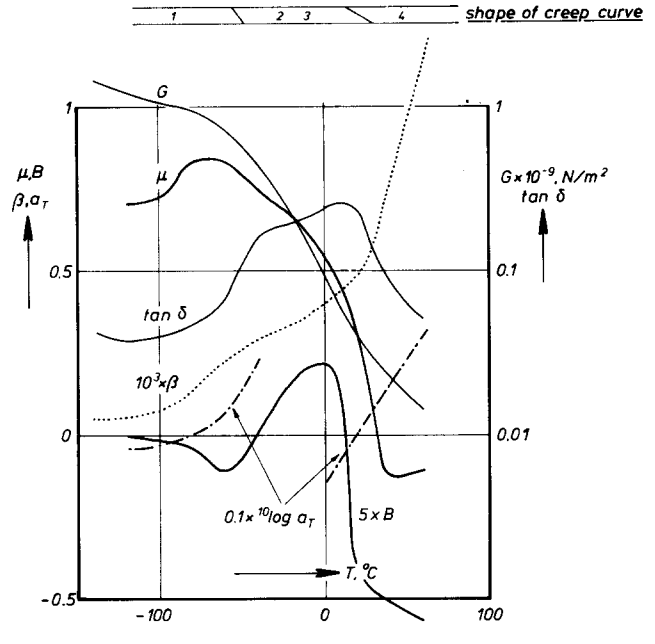

Figure 20 As for *Figure 19*, but now for LDPE (41), quenched from 80°C

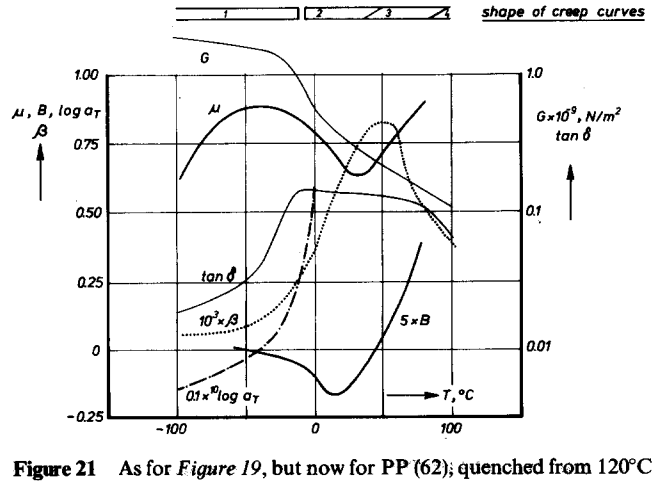

Figure 21 As for *Figure 19*, but now for PP (62), quenched from 120°C

In *Figures 19–24* some specific materials are highlighted and the following remarks relate to these materials:

(a) For PP, the Figures give only data on the high-molecular weight material nr. 62; the other polypropylenes behave very similarly.

(b) For nylon-6, the behaviour of the nucleated and unnucleated samples was very similar, and only the data on the nucleated polymer are presented (see *Figure 23*). A

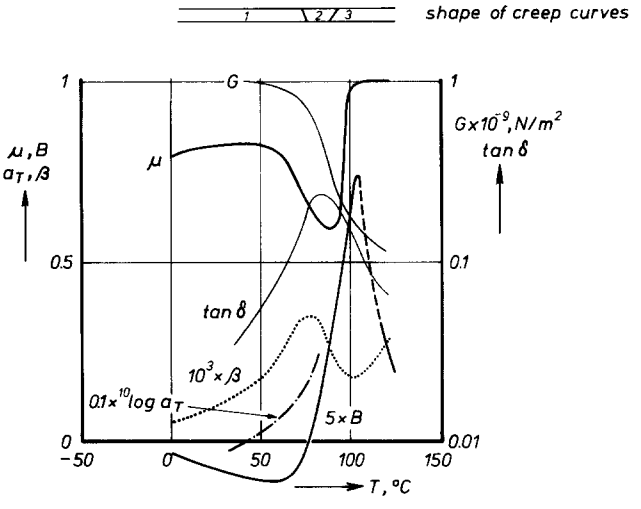

Figure 22 As for *Figure 19*, but now for PET (37), quenched from 140°C

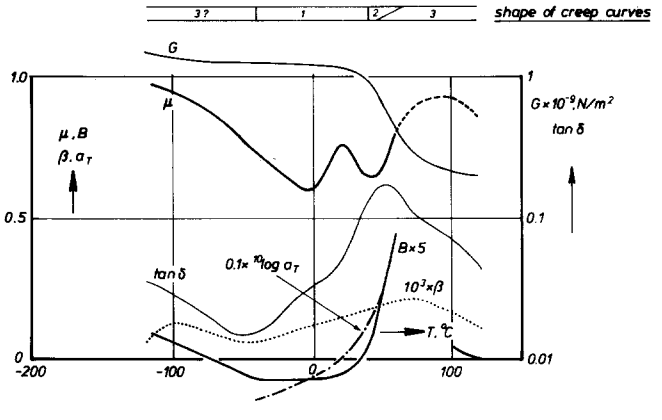

Figure 23 As for *Figure 19*, but now for nylon-6 (59), quenched from 150°C

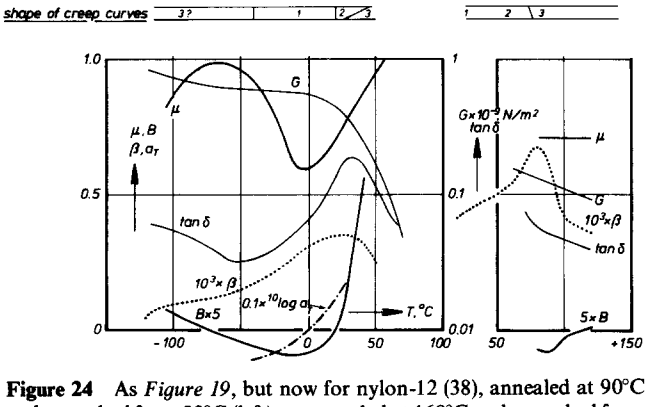

Figure 24 As *Figure 19*, but now for nylon-12 (38), annealed at 90°C and quenched from 80°C (left), or annealed at 160°C and quenched from 140°C (right)

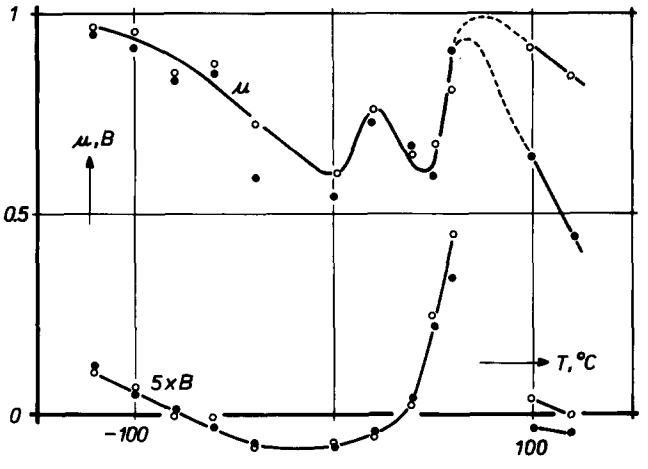

Figure 25 Shift rates μ and B for nucleated nylon-6 (59) (○), and unnucleated nylon-6 (60) (●), both annealed at 160°C and quenched from 150°C

comparison of the two types of nylon-6 is given in *Figure 25*; the main effect of nucleation is an increase in crystallinity (see *Table 1*) accompanied by more marked ageing effects at $T > 50$°C.

(c) For nylon-12, *Figure 24* shows two sets of data. The first relates to the polymer annealed at 90°C and quenched from 80°C; the second set was obtained after annealing at 160°C, which clearly causes a considerable increase in crystallinity (compare *Table 1*, and also, in *Figure 24*, the magnitude of the moduli).

Let us now compare *Figures 19–24* with the model predictions in *Figure 8* by considering the materials individually.

HDPE (Figure 19)

The picture agrees almost perfectly with that of *Figure 8*. T_g^L is estimated to be about -40°C and even at $+60$°C the glass transition is still not completed (at least for creep times of the order of 1000 s).

LDPE (Figure 20)

T_g^L and T_g^U are much closer to each other than for HDPE; T_g^L is about -60°C, and T_g^U is found around room temperature. As a consequence, the transition from Regions 1 to 4 occurs in a relatively narrow temperature range, and Regions 2 and 3 are no longer well separated. This may explain why there is no minimum in the μ vs. T curve, and why it is difficult to decide whether the creep curves are of type 2 or type 3 (see *Figure 20*).

The fact that the T_g^U of LDPE is much lower than that of HDPE implies that the amorphous phase is less immobilized, which agrees with expectations. The decrease in immobilization also implies that the lower glass transition becomes more marked than in HDPE. Comparison of the damping curves of *Figures 19* and *20* reveals that this is indeed the experimental situation.

A complication with LDPE is the ageing at temperatures above 20°C, i.e. in Region 4. According to our model, crystallization processes may occur and cause ageing in this region, and for the following reasons we believe that this is indeed what actually happens:

(1) The shifts in the creep curves are almost vertical; μ even becomes negative.

(2) The volume sensitivity $\mathrm{d}\ln J/\mathrm{d}\ln v$ of the compliance is much smaller than in Regions 1–3. It can be calculated by dividing the rate $\mathrm{d}\ln J/\mathrm{d}\ln t_e$ (due to ageing) by the volume relaxation rate $\mathrm{d}\ln v/\mathrm{d}\ln t_e$. We then find that, at 40°C and 60°C, $\mathrm{d}\ln J/\mathrm{d}\ln v$ is about 100, whereas at -60°C it is no less than 520. The low value of 100 is much nearer the value of $\mathrm{d}\ln J/\mathrm{d}\ln v$ obtained when the material is stiffened by annealing at high temperatures[15] (changes in crystallinity).

Polypropylene (Figure 21)

The picture again agrees perfectly with the theory given in *Figure 8*. As expected, T_g^L is found between -20°C and 0°C, and T_g^U lies above 80°C.

Poly(ethylene terephthalate)

In PET, the glass transition at about 80°C is very pronounced. This explains the fact that the vertical shift rate B passes a sharp maximum, and that just above T_g the ageing effects cannot be deconvoluted into horizontal and vertical shifts (see *Figure 7b*).

Nylon-6 and nylon-12 (Figures 23 and 24)

Since the behaviour of these two polymers is rather similar, we will only discuss that of nylon-6. As for PET, the transition around 50°C is very pronounced; the shift rate B passes a maximum and just above the transition, i.e. at 80°C, the ageing effects cannot be deconvoluted into shifts (see *Figure 14*). T_g^U lies far above 100°C, and for $T > 100$°C, the creep rate of the more mobile and now rubbery regions appears to be very small. For this reason, ageing at 100°C–120°C produces shifts that are almost horizontal (see *Figure 26*).

The small peak in μ at 20°C appears to be real. It is observed in both types of nylon-6 (see *Figure 25*) and also in a nylon-6 sample investigated previously (data not shown). The origin of the peak is not clear. An interesting point is the behaviour of the nylons at low temperatures ($T < -40$°C). In *Figures 23* and *24* we observe many aspects of a type 3 behaviour: the value of μ is large, the creep curves have the requisite shape, and time–temperature superposition is impossible (see *Figure 27*). This suggests that, somewhat below -100°C, there is another glass transition. The peaks in tan δ and in volume

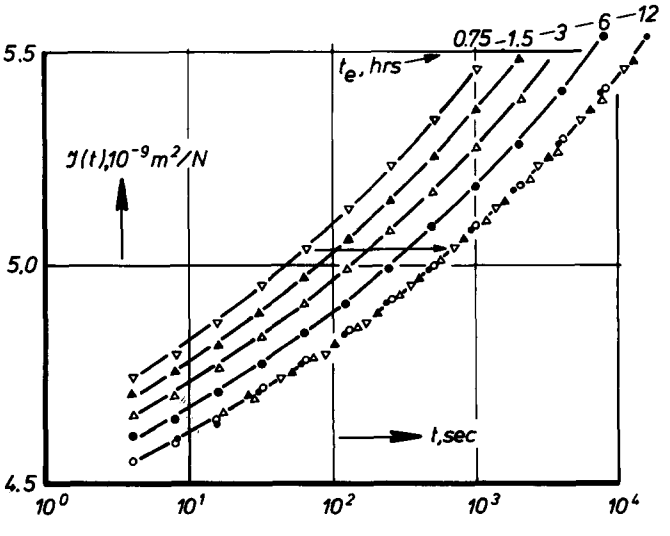

Figure 26 Small-strain torsional creep of nylon-6 (59), at various values of time t_e elapsed after a quench from 150°C to 120°C. The master curve was obtained by purely horizontal shifting

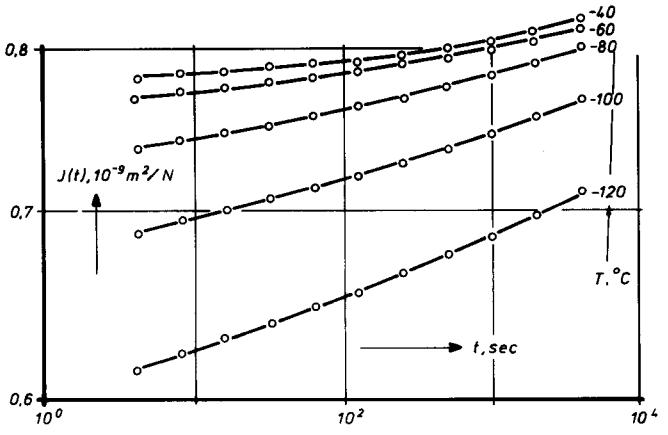

Figure 27 Torsional creep of nylon-6 (59), 3 h after quenches from 150°C to T

relaxation rate β suggest the same (*Figures 23* and *24*). It is unlikely that the transition around −100°C is a secondary transition (local relaxation mode) because at secondary transitions μ usually decreases to zero[1]; for the nylons μ remains at about unity down to −120°C. Further support for a low temperature glass transition is found in the very low value of the modulus of nylon-12 between −100°C and 0°C.

DISCUSSION

As stated in the Introduction, the general discussion of the results is postponed to a later paper in the series. Here it suffices to say that the predictions of the model are in agreement with experiment, even in detail. All materials show the four characteristic types of behaviour, which, with increasing temperature, appear in the correct order. Only for the nylons is there an unexplained extra ageing at low temperatures.

CONCLUSION

The creep and ageing behaviour of semicrystalline polymers can be explained from a model of a glass transition extended towards the high-temperature side.

ACKNOWLEDGEMENTS

The author wishes to acknowledge Akzo, ANIC, BP-Chemicals, DSM, Chem. Werke Hüls, Montedison, Rhône-Progil and Shell for sponsoring the work during the years 1973/74 when most of the results reported here were obtained. Moreover, he is greatly indebted to Mrs C. Zoeteweij, Mrs M. P. Bree and Mrs E. P. M. Kerklaan for carefully performing the experiments, and to Mr G. A. Gerritse for the preparation of the rubber samples.

REFERENCES

1 Struik, L. C. E. 'Physical Aging of Amorphous Polymers and other Materials', Elsevier, Amsterdam, 1978
2 Smit, P. P. A. *Rheol. Acta* 1966, **5**, 277
3 Schwarzl, F. R. *et al. Rheol. Acta* 1966, **5**, 270
4 Kraus, G. *Adv. Polym. Sci.* 1971, **8**, 155
5 Struik, L. C. E. *Plastics Rubber Process. Appl.* 1982, **2**, 41
6 Schael, G. W. *J. Appl. Polym. Sci.* 1966, **10**, 901
7 Gezovich, D. M. and Geil, P. M. *Polym. Eng. Sci.* 1968, **8**, 202
8 Gezovich, D. M. and Geil, P. M. *Polym. Eng. Sci.* 1968, **8**, 210
9 Kapur, S. and Rogers, C. E. *J. Polym. Sci.* 1972, **10**, 2107
10 Turner, S. *Plastics Polym.* 1970, **38**, 282
11 Dunn, C. M. R. and Turner, S. *Polymer* 1974, **15**, 451
12 Miller, R. L. in 'Encyclopedia of Polymer Science and Technology', Vol. 4 (Ed. N. Bikales), Wiley, New York, 1966
13 Schwarzl, F. R. and Struik, L. C. E. *Adv. Mol. Relaxation Processes* 1967–68, **1**, 201
14 Struik, L. C. E. *Polymer* 1980, **21**, 962
15 Ogorkiewicz, R. M. 'Engineering Properties of Thermoplastics', Wiley–Interscience, London, 1970